

AperTO - Archivio Istituzionale Open Access dell'Università di Torino

Use of poly(DL-lactide- ϵ -caprolactone) membranes and mesenchymal stem cells from the Wharton's jelly of the umbilical cord for promoting nerve regeneration in axonotmesis: In vitro and in vivo analysis.

This is the author's manuscript

Original Citation:

Availability:

This version is available <http://hdl.handle.net/2318/125555> since 2016-06-13T15:07:52Z

Published version:

DOI:10.1016/j.diff.2012.10.001

Terms of use:

Open Access

Anyone can freely access the full text of works made available as "Open Access". Works made available under a Creative Commons license can be used according to the terms and conditions of said license. Use of all other works requires consent of the right holder (author or publisher) if not exempted from copyright protection by the applicable law.

(Article begins on next page)



UNIVERSITÀ DEGLI STUDI DI TORINO

This is an author version of the contribution published on:

Questa è la versione dell'autore dell'opera:

Differentiation. 2012 Dec;84(5):355-65. doi: 10.1016/j.diff.2012.10.001. Epub 2012 Nov 7.

The definitive version is available at:

La versione definitiva è disponibile alla URL:

<http://www.sciencedirect.com/science/article/pii/S0301468112001429>

Use of poly(DL-lactide-e-caprolactone) membranes and mesenchymal stem cells from the Wharton's jelly of the umbilical cord for promoting nerve regeneration in axonotmesis: In vitro and in vivo analysis

A. Gartner, T. Pereira, P.A.S. Armada-da-Silva, I. Amorim, R. Gomes, J. Ribeiro, M.L. Franca, C. Lopes, B. Porto, R. Sousa, A. Bombaci, G. Ronchi, F. Fregnan, A.S.P. Varejao, A.L. Lui's, S. Geuna, A.C. Mauricio

Abstract

Cellular systems implanted into an injured nerve may produce growth factors or extracellular matrix molecules, modulate the inflammatory process and eventually improve nerve regeneration. In the present study, we evaluated the therapeutic value of human umbilical cord matrix MSCs (HMSCs) on rat sciatic nerve after axonotmesis injury associated to Vivosorbs membrane. During HMSCs expansion and differentiation in neuroglial-like cells, the culture medium was collected at 48, 72 and 96 h for nuclear magnetic resonance (NMR) analysis in order to evaluate the metabolic profile. To correlate the HMSCs ability to differentiate and survival capacity in the presence of the Vivosorbs membrane, the $[Ca^{2+}]_i$ of undifferentiated HMSCs or neuroglial-differentiated HMSCs was determined by the epifluorescence technique using the Fura-2AM probe. The Vivosorbs membrane proved to be adequate and used as scaffold associated with undifferentiated HMSCs or neuroglial-differentiated HMSCs. In vivo testing was carried out in adult rats where a sciatic nerve axonotmesis injury was treated with undifferentiated HMSCs or neuroglial differentiated HMSCs with or without the Vivosorbs membrane. Motor and sensory functional recovery was evaluated throughout a healing period of 12 weeks using sciatic functional index (SFI), extensor postural thrust (EPT), and withdrawal reflex latency (WRL).

Stereological analysis was carried out on regenerated nerve fibers. In vitro investigation showed the formation of typical neuroglial cells after differentiation, which were positively stained for the typical specific neuroglial markers such as the GFAP, the GAP-43 and NeuN.

NMR showed clear evidence that HMSCs expansion is glycolysis-dependent but their differentiation requires the switch of the metabolic profile to oxidative metabolism. In vivo studies showed enhanced recovery of motor and sensory function in animals treated with transplanted undifferentiated and differentiated HMSCs that was accompanied by an increase in myelin sheath. Taken together, HMSC from the umbilical cord Wharton jelly might be useful for improving the clinical outcome after peripheral nerve lesion.

1. Introduction

A full understanding of nerve regeneration, especially complete functional achievement and organ reinnervation after nerve injury, still remain the principle goal of regenerative medicine. The reliability of animal models is crucial for peripheral nerve research. Because of its peripheral nerve size, the rat sciatic nerve has been the most commonly experimental model used in studies concerning the peripheral nerve regeneration and possible therapeutic approaches (Ronchi et al., 2009). Although sciatic nerve injuries are rare in humans, this experimental model provides a very realistic testing bench for lesions involving plurifascicular mixed nerves with axons of different size and type competing to reach and reinnervate distal targets (Amado et al., 2008; Mackinnon et al., 1985). Focal crush causes axonal interruption but preserves the connective sheaths (axonotmesis). After this kind of injury, regeneration is usually successful, in a short latency (1–2 days), axons regenerate at a steady rate along the distal nerve supported by the reactive Schwann cells (SCs) and the preserved endoneurial tubules which enhance axonal elongation and facilitate adequate reinnervation (Luis et al., 2007).

Tissue engineering of peripheral nerves associates biomaterials, like chitosan, PLC, and other biomaterials, some of them, previously studied by our group (Amado et al., 2008; Luis et al., 2008a; Maurício et al., 2011) to cellular systems, able to differentiate into neuroglial like cells or even by modulating the inflammatory process, which might improve nerve regeneration, in terms of motor and sensory recovery, and also, by shortening the healing period avoiding regional muscular atrophy. Cell

transplantation has been proposed as a method of improving peripheral nerve regeneration (Chen et al., 2007). SCs, MSCs, embryonic stem cells, marrow stromal cells are the most studied support cells candidates. Schwann cell transplantation enhances axon outgrowth both in vitro (Schlosshauer et al., 2003) and in vivo (Keilhoff et al., 2006). Transplantation of viable SCs offers better results than the sheer release of growth factors, because SCs have the above mentioned regeneration promoting effect (Bhatheja and Field, 2006; Fansa et al., 1999; Hall, 1978; Ide, 1996; Madduri and Gander, 2010; Muir, 2010; Schmitte et al., 2010). The generation of sufficient amounts of SCs for auto-transplantation, however, requires a significant time for cell culture. Current concepts include mitogenic substances to enhance cell yield. Due to their side effects they should be avoided in clinical therapy. Moreover, functional nerves have to be sacrificed as SCs donor resulting in loss of sensation, scarring and, possibly, neuroma formation. The limitations of harvesting autologous SCs, such as donor nerve sacrifice and donor site morbidity, have led to investigation of other cell types that provide similar trophic support to axon regeneration (Ladak et al., 2011).

On the other hand, MSCs have become one of the most interesting targets for Tissue Regeneration including the peripheral nerves. Like bone marrow stromal cells and other mesenchymal cells, they are plastic adherent, stain positively for markers of the mesenchymal (CD10, CD13, CD29, CD44, CD90, and CD105) and negatively for markers of the hematopoietic lineage (Wang et al., 2004). These cells are capable of self-renewal with sustained proliferation in vitro and can differentiate into multiple mesodermal cells, including neuron-like cells (Park et al., 2010). The high plasticity and low immunogenicity of these cells, turn them into a desirable form of cell therapy for the injured nervous system without requiring the use of immunosuppressive drugs during the treatments (Thuret et al., 2006). MSCs have been isolated from various other origins, including skin, hair follicle, periosteum, amniotic fluid, umbilical cord blood and adipose tissue. Harvest and expansion of MSCs are straight forward techniques (Colter, 2000; Gnecci and Melo, 2009), which are not only feasible regarding the laboratory approach but also regarding their application with the patient. With appropriate stimuli and environmental conditions MSCs exhibit a respectable plasticity (Joshi and Enver, 2002). They may even differentiate into non-mesenchymal lineages, including myelinating cells of the peripheral nervous system (PNS) (Dezawa et al., 2001; Tohill et al., 2004). Beside their easy expansion in culture their plasticity makes MSCs an ideal source for tissue repair and tissue engineering. Bone marrow represents the most commonly used tissue source of adult MSCs. Bone marrow MSCs (BMSCs) have been applied for cell based therapies; however, due to the limited number of BMSCs available for autologous use and the possibility of donor site morbidity and the decreased number of BMSCs along the adult life, there is a need to identify alternative MSCs sources.

A recently reported potential alternative tissue source of MSCs is the connective tissue (Wharton's Jelly) of human umbilical cord (UC). Different harvesting procedures have led to UC-derived cells that exhibit a neuronal phenotype (Fu et al., 2006; Mitchell et al., 2003; Sarugaser et al., 2005; Wang et al., 2004) and have potential utility in treatment of neurodegenerative diseases (Weiss et al., 2003, 2006), indicating the versatility of this cell source. Interestingly, these cells, which are major histocompatibility complex (MHC) class II negative, not only express immunoprivileged and immunomodulatory phenotype, but also their MHC class I expression levels can be manipulated (Sarugaser et al., 2005), making them a potential cell source for MSC-based therapies. In addition, these cells represent a non controversial source of primitive mesenchymal progenitor cells that can be harvested after birth, cryogenically stored, thawed, and expanded for therapeutic uses (Mauricio et al., 2011).

The aim of this study was to explore the therapeutic value of human UC matrix (Wharton's jelly) derived MSCs (HMSC) both in vitro and in vivo, associated to a Poly(DL-lactide-ε-caprolactone) PLC (Vivosorbs) membrane, on a rat sciatic nerve axotomy experimental model.

2. Materials and methods

2.1. Poly(DL-lactide-ε-caprolactone) (PLC) membranes

Poly(DL-lactide-ε-caprolactone) (PLC) membranes (Vivosorbs) were purchased from Polyganics BV, Groningen, Netherlands (FS01-006/20 Lot: FSA2009092311).

2.2. Cell culture and in vitro differentiation of HMSC from Wharton's jelly umbilical cord

Human MSC from Wharton's jelly UC (HMSCs) were purchased from PromoCell GmbH (C-12971, lot-number: 8082606.7). Cryo-preserved cells were cultured and maintained in a humidified atmosphere with 5% CO₂ at 37 °C. Mesenchymal Stem Cell Medium (PromoCell, C-28010) was replaced every 48 h. At 90% confluence, cells were harvested with 0.25% trypsin with EDTA (Gibco) and passed into a new flask for further expansion. HMSCs at a concentration of 2500 cell/ml were cultured and after 24 h cells exhibited 30–40% confluence. Differentiation was induced with MSC neurogenic medium (Promocell, C-28015). Medium was replaced every 24 h for 3 days. The formation of neuroglial-like cells was observed after 24 h in an inverted microscope (Zeiss, Germany).

Intracellular free Ca²⁺ concentration ([Ca²⁺]_i) was measured in Fura-2-loaded cells by using dual wavelength spectrofluorometry as previously described (Amado et al., 2008). The measurements were performed on undifferentiated HMSCs after confluence was obtained and on neuroglial-differentiated HMSCs, cultured on Vivosorbs discs in order to correlate the HMSCs ability to differentiate and survival capacity in the presence of the Vivosorbs membrane.

2.3. Cytogenetic analysis of human MSC from Wharton's jelly

HMSC cell line (differentiated) from Wharton's jelly was studied for cytogenetic analysis at passage 5. When confluence was reached, culture medium was changed and supplemented with 4 mg/ml colcemid solution (stock solution, Cat. No. 15212-012, Gibco). After 4 h, HMSCs were collected and suspended in 8 ml of 0.075 M KCl solution supplemented with bovine fetal serum (BFS). Then the suspension was incubated at 37 °C for 35 min. After centrifugation (1500 rpm), 8 ml of the fixative methanol: glacial acetic acid at 6:1 was added and mixed together, and the cells were again centrifuged. After two rounds of fixation, two new rounds were performed with the fixative methanol: glacial acetic acid at 3:1. After the last centrifugation, the HMSC suspension was spread onto very well glass cleaned slides. Analysis was performed by one scorer on Giemsa-stained cells.

2.4. Immunocytochemistry

At passage 3, HMSCs were trypsinized, washed and re-suspended in Mesenchymal Stem Cell Medium (PromoCell, C-28010) at a concentration of 1 × 10⁵ cell/ml. HMSCs were fixed with paraformaldehyde at 4 °C for 15 min and washed with distilled water before permeabilization in 0.5% Triton-X100. Non-specific binding was blocked using blocking solution (PBS containing 1% bovine serum albumin (BSA)) for 1 h at room temperature. HMSCs were then incubated for 2 h at room temperature with primary antibodies of rabbit anti-growth associated protein-43 (GAP-43, 1:200) (Chemicon, AB5220), rabbit anti-glial fibrillary acidic protein (GFAP, 1:500) (Chemicon, AB5804) and mouse anti-neuronal nuclei (NeuN, 1:100) (Chemicon, MAB377). After washing, HMSCs were incubated 15 min with secondary antibodies goat anti-rat IgG (Millipore, AP136P) and goat anti-rabbit IgG (Millipore, 12-348MN). After several washes in PBS, HMSCs were incubated with horseradish peroxidase (HRP)-coupled streptavidin for 10 min. DAB (diamino-benzidine) served as chromogen.

2.5. NMR spectroscopy

During HMSCs expansion and differentiation to neuroglial-like cells, 160 mL of the culture medium was collected at 48, 72 and 96 h (N=45) for nuclear magnetic resonance (NMR) analysis. ¹H-NMR spectra of the collected samples were acquired at 14.1 T, 25 °C, using a Varian 600 MHz spectrometer equipped with

a 3 mm indirect detection probe with z-gradient (Varian, Palo Alto, CA) by standard methods. Solvent-suppressed ^1H -NMR spectra were acquired with 6 kHz sweep width, using 14 s delay for allowing total proton relaxation, 3 s water pre-saturation, 451 pulse angle, 3.5 s acquisition time, and at least 64 scans. ^1H -NMR spectroscopy was performed and the following metabolites were determined: lactate, doublet located at 1.33 ppm; alanine, doublet at 1.45 ppm; and H1- α glucose, doublet at 5.22 ppm. Sodium fumarate (final concentration of 2 mM) was used as an internal reference (6.50 ppm) to quantify metabolites in solution. The relative areas of ^1H -NMR resonances were quantified using the curve-fitting routine supplied with the NUTSproTM NMR spectral analysis program (Acorn, NMR Inc, Fremont, CA).

2.6. Surgical procedure

For the *in vivo* testing, Sasco Sprague adult rats (Charles River Laboratories, Barcelona, Spain) were divided in groups of 6 animals each: a group of 6 animals was used as control without any sciatic nerve injury (Group 1 – Control). In Group 2 the crushed sciatic nerve did not have any other intervention (Group 2 – Crush). In Group 3, the axonotmesis lesion of 3 mm was enwrapped with a PLC (Vivosorbs) membrane (Group 3 – CrushPLC). In Group 4, the crushed sciatic nerve was infiltrated in the lesion area with a suspension of 1500 HMSCs (in a total volume of 50 μl) (Group 4 – CrushCell), in Group 5, the crushed sciatic nerve was encircled by a PLC (Vivosorbs) membrane covered with a monolayer of non (Group 5 – CrushCellNonDifPLC) and in Group 6 the axonotmesis lesion of 3 mm was enwrapped with a PLC (Vivosorbs) membrane covered with a monolayer of differentiated HMSCs (neuroglial-like cells) (Group 6 – CrushCell-DifPLC). The standardized crush injury was carried out with the animals placed prone under sterile conditions and the skin from the clipped lateral right thigh scrubbed in a routine fashion with antiseptic solution. The surgery procedure was the one previously described (Lui's et al., 2007; Luis et al., 2007). The standard crush injury was performed by a non-serrated clamp (Institute of Industrial Electronic and Material Sciences, University of Technology, Vienna, Austria), exerting a constant force of 54 N for a period of 30 s, 10 mm above the bifurcation into tibial and common peroneal nerves inducing a 3 mm axonotmesis lesion. To prevent autotomy, a deterrent substance was applied to rat right foot. No local or systemic signs of rejection or foreign body were observed in the experimental animals transplanted with PLC membranes and HMSCs. There was no need of administering immunosuppressive treatment to the experimental animals during the entire healing period of 12 weeks after the surgical procedure.

2.7. Functional assessment

All animals were tested preoperatively (week 0), and every week until the end of the 12-week follow-up time.

2.7.1. Motor performance and nociceptive function

Motor performance and nociceptive function were evaluated by measuring extensor postural thrust (EPT) and withdrawal reflex latency (WRL), respectively (Luis et al., 2007, 2008a, b). For EPT test, the affected and normal limbs were tested 3 times, with an interval of 2 min between consecutive tests, and the 3 values were averaged to obtain a final result. The normal (unaffected limb) EPT (NEPT) and experimental EPT (EEPT) values were incorporated into an equation (Eq. (1)) to derive the percentage of functional deficit, as described in the literature (Koka and Hadlock, 2001)

$$\% \text{Motor deficit} = \frac{1}{2} \left(\frac{\text{NEPT} - \text{EEPT}}{\text{NEPT}} \right) \times 100 \quad (1)$$

The nociceptive withdrawal reflex (WRL) was adapted from the hotplate test developed by Masters et al. (1993) and described elsewhere (Luis et al., 2007, 2008a, b). Normal rats withdraw their paws from the hotplate within 4 s or less (Hu et al., 1997). The cutoff time for heat stimulation was set at 12 s to avoid skin damage to the foot (Varejao et al., 2003).

2.7.2. Sciatic functional index (SFI)

For SFI, animals were tested in a confined walkway measuring 42 cm long and 8.2 cm wide, with a dark

shelter at the end, as previously described (Luis et al., 2007, 2008a, b). Several measurements were taken from the footprints: (i) distance from the heel to the third toe, the print length (PL); (ii) distance from the first to the fifth toe, the toe spread (TS); and (iii) distance from the second to the fourth toe, the intermediary toe spread (ITS). For SFI, all measurements were taken from the experimental (E) and normal (N) sides. The mean distances of three measurements were used to calculate the following factors:

Toe spread factor (TSF) $\frac{1}{4} \frac{(ETS - NTS)}{NTS}$

Intermediate toe spread factor (ITSF) $\frac{1}{4} \frac{(EITS - NITS)}{NITS}$ Print length factor (PLF) $\frac{1}{4} \frac{(EPL - NPL)}{NPL}$

SFI was calculated as described by Bain et al., (1989) according to the following equation:

$SFI = \frac{1}{4} \left[\frac{EPL - NPL}{NPL} + \frac{ETS - NTS}{NTS} \right]$

$\frac{1}{4} \left[\frac{EITS - NITS}{NITS} + \frac{EPL - NPL}{NPL} \right]$

$\frac{1}{4} \left[\frac{ETS - NTS}{NTS} + \frac{EITS - NITS}{NITS} \right]$

For SFI, an index score of 0 is considered normal and an index of ≥ 100 indicates total impairment. When no footprints were measurable, the index score of ≥ 100 was given (Dijkstra et al., 2000).

2.8. Sciatic nerve stereology

Nerve samples (10-mm-long sciatic nerve segments distal to the crush site and from un-operated controls) were processed for quantitative morphometry of myelinated nerve fibers (Raimondo et al., 2009). Fixation was carried out using 2.5% purified glutar-aldehyde and 0.5% saccharose in 0.1 M Sorensen phosphate buffer for 6-8 hours and resin embedding was obtained following Glauerts' procedure (Scipio et al., 2008). Series of 2-mm thick semi-thin transverse sections were cut using a Leica Ultracut UCT ultramicrotome (Leica Microsystems, Wetzlar, Germany) and stained by Toluidine blue. Stereology was carried out on a DM4000B microscope equipped with a DFC320 digital camera and an IM50 image manager system (Leica Microsystems, Wetzlar, Germany). Systematic random sampling and D-disector were adopted using a protocol previously described (Geuna et al., 2000, 2004). Fiber density and total number of myelinated fibers were estimated together with fiber and axon diameter and myelin thickness.

2.9. Statistical analysis

Data of functional tests are reports as means and standard deviations (SD) at each time point, including pre-operatively, and each experimental group. Differences between time points and between groups were tested by two-way analysis of variance (ANOVA) using a mixed model of within (time of recovery) and between-subjects (experimental groups) factors. In cases of significant main effect of experimental group (between-subjects factor), pairwise comparisons were further conducted using the post hoc Tukey's HSD test using IBM SPSS statistics19 software package (SPSS, Inc.). For stereology, statistical comparisons of quantitative data were subjected to one-way ANOVA test using the software "Statistica per discipline biomediche" (McGraw-Hill, Milan, Italy). In RMN studies, comparison of data between different experimental groups was performed by One-way ANOVA followed by Newman-Keuls post-hoc test using GraphPad Prism Software, (San Diego California USA). In all cases differences at $p < 0.05$ were considered significant.

3. Results

3.1. Cytocompatibility of Vivosorbs membranes and confirmation of HMSCs differentiation into neuroglial-like cells and karyotype analysis.

Results obtained from epifluorescence technique are referred to measurements from undifferentiated HMSCs and neuroglial-differentiated HMSCs which correspond to $[Ca^{2+}]_i$ from cells that did not begin the apoptosis process (data not shown). The undifferentiated HMSCs cultured on Vivosorbs membranes reached confluence and exhibited a normal star-like shape with a flat morphology in culture. In the presence of neurogenic medium, the formation of neuroglial-like cells was observed after 24 h. According to these results, it is reasonable to conclude that Vivosorbs membranes are a viable substrate for undifferentiated HMSCs culture or neuroglial-differentiated HMSCs adhesion, multiplication and differentiation.

The phenotype of HMSCs was assessed by PromoCell. Rigid quality control tests are performed for each lot of PromoCell HMSCs isolated from Wharton's jelly of UC. HMSCs were tested for cell morphology,

adherence rate and viability. Furthermore, for each cell lot of characterization was characterized by flow cytometry analysis for a comprehensive panel of markers, such as PECAM (CD31), HCAM (CD44), CD45, and Endoglin (CD105). The HMSCs exhibited a mesenchymal-like shape with a flat and polygonal morphology. During the expansion of cells long spindle-shaped and colonized the whole culturing surface was observed (Fig. 1A). After 96 h of culture in neurogenic medium, we observed a morphological change. The cells became exceedingly long and there was a formation of typical neuroglial-like cells with multi-branches and secondary branches (Fig. 1B). The differentiation was tested based on the expression of typical neuronal markers such as GFAP, GAP-43 and NeuN in neuroglial-like differentiated MSCs. Undifferentiated HMSCs were negatively labeled to GFAP, GAP-43 and NeuN (Fig. 2A, C and E, respectively). After 96 h of differentiation the attained cells were positively stained for glial protein GFAP (Fig. 2B) and for the growth-associated protein GAP-43 (Fig. 2D). All nuclei of neuroglial-like cells were also labeled with the neuron specific nuclear protein NeuN (Fig. 2E) demonstrating successful differentiation of HMSCs in neuroglial-like cells.

Undifferentiated HMSCs exhibited a normal star-like shape with a flat morphology. After in vitro differentiation, HMSCs morphology changed into typical neuroglial-like pattern with multi-branches and secondary branches (Fig. 1B). Giemsa-stained cells of differentiated HMSC cell line at passage 5 were analyzed for cytogenetic characterization. However, no metaphases were found, therefore the karyo-type could not be established. The karyotype of undifferentiated HMSCs was determined previously and no structural alterations were found demonstrating absence of neoplastic characteristics in these cells, as well as chromosomal stability to the cell culture procedures.

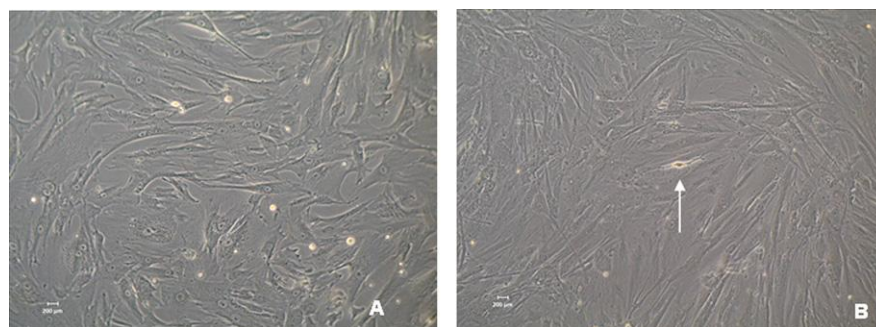


Fig. 1. HMSCs from Wharton's jelly exhibiting a mesenchymal-like shape with a flat polygonal morphology (A). After 72 h of culture in neurogenic medium the cells became exceedingly long and there is a formation of typical neuroglial-like cells with multibranched. (B) (Magnification: 100x).

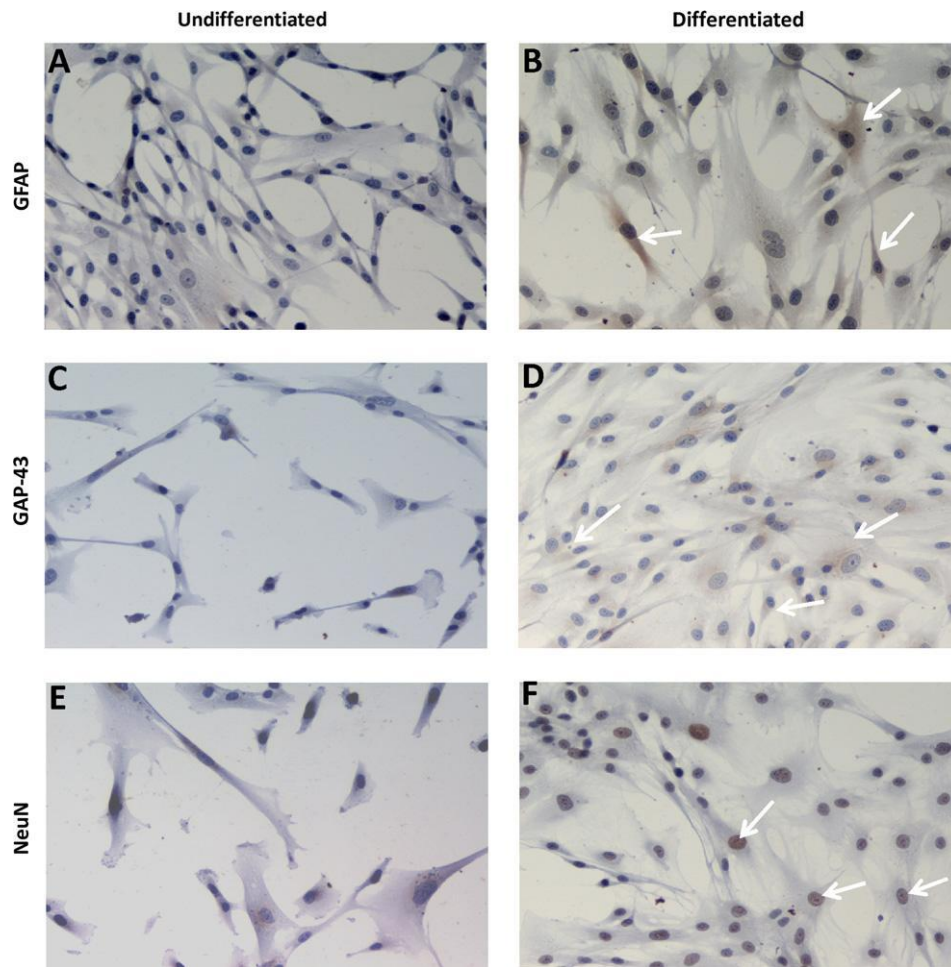


Fig. 2. Undifferentiated HMSC cells from the Wharton's jelly presenting a negative staining for: (A) GFAP which is a glial cell marker, (C) GAP-43 which is related with axonal outgrowth, and (E) NeuN which is a marker for nucleus of neurons. Neuroglial-like cells obtained from HMSCs in vitro differentiated with neurogenic medium exhibiting a positive staining for: (B) GFAP, (D) GAP-43, and (F) NeuN (Magnification: 200x).

3.2. Glycolysis is stimulated during HMSCs expansion but not during differentiation

During the 96 h expansion of undifferentiated HMSCs, the glucose consumption was 4.470.05 pmol/cell, while during differentiation the cells consumed 5.071.1 pmol/cell. Interestingly, although the glucose consumption was very similar in both conditions after the 96 h cell culture, the glucose consumption rate was only similar between the 48 and 72 h. Undifferentiated HMSCs mostly consumed glucose in the first 48 h at a rate of 0.570.004 pmol/h/cell/h, while during differentiation, the glucose consumption rate lowered to just 0.0870.01 pmol/h/cell/h. Between the 72 and 96 h of culture, the glucose consumption was also increased in undifferentiated cells (0.2170.04 pmol/h/cell) when compared with cells undergoing differentiation (0.0870.04 pmol/h/cell). As expected, the lactate production increased during HMSCs expansion. After 96 hours, the lactate production was 2671.1 pmol/cell during expansion, while during cell differentiation the total lactate production was 6.07 0.6 pmol/cell. The lactate production rate during HMSCs expansion was increased during the first and last hours of expansion. In the first 48 h, the rate was 0.270.03 pmol/h/cell and between the 72 and 96 h the rate was 0.570.04 pmol/h/cell. Interestingly, during the 96 h of differentiation the lactate production rate was almost stable although between the 48 and 96 h of differentiation there was no production but a slight consumption of lactate.

3.3. Lactate and alanine metabolism is altered during differentiation of HMSCs

Alanine production was significantly decreased during HMSCs differentiation. During the 96 h expansion, the cells produced 6.97 0.7 pmol/cell while after differentiation the alanine production was 2.270.4 pmol/cell. During expansion and differentiation, the alanine was mostly produced during the first hours as seen by the alanine production rate. During the first 48 h, undifferentiated HMSCs produced alanine at a rate of 0.1070.003 pmol/h/cell while during differentiation, in that period, the alanine production rate was 0.0270.008 pmol/h/cell. The lactate/alanine ratio was significantly decreased after 48 and 72 h in undifferentiated HMSCs. The ratio decreases from 3.570.3 at time zero of expansion to 2.170.1 and 2.570.3 in the following 48 and 72 h, respectively. After 96 h, HMSCs differentiated into neuroglial-like cells presented a significantly lower lactate/alanine ratio (2.670.5) than undifferentiated cells (3.970.2).

3.4. Functional analysis

3.4.1. Nociceptive function evaluated by withdrawal reflex latency (WRL)

The withdrawal reflex requires intact thermal and nociceptive innervations of the hindpaw. Early after sciatic axonotmesis, the withdrawal response could not be recorded and WRL values rose to the cutoff time of 12 s (Table 1). WRL progressively reduced approaching the normal values at week 12. There was a significant effect of time in WRL scores during the healing period [$F(10,330)=168.32$, $p<0.000$]. An overall main effect of kind of treatment was also noticed in WRL results during the healing time [$F(5,33)=422.786$, $p<0.000$]. WRL values were significantly different in groups treated with the PLC membrane, alone or in combination with undifferentiated and differentiated HMSCs (Group 5 – CrushCellNonDifPLC; Group 6 – CrushCellDifPLC; Group 3 – CrushPLC) with the groups not receiving the PLC membrane ($p<0.05$). In this case, however, the WRL values seem to indicate better functional recovery in the groups with the cellular system (Group 5 – CrushCellNonDifPLC; Group 6 – CrushCellDifPLC), demonstrating the positive results concerning the cellular system treatment (Table 1).

3.4.2 Motor performance by measuring extensor postural thrust (EPT)

The EPT measures the antigravity response when animals are lowered and the hindlimb is loaded. In control animals and before injury, EPT scores center around zero, showing similar forces in both sides. In the week following sciatic axonotmesis, EPT scores increased to near maximal values, indicating almost complete loss of contractile force in the affected hindlimb. EPT scores then recovered steadily in the following weeks to normal values. Therefore, a significant effect of time in EPT scores during the

healing period was found [$F(10,330)=136.09$, $p<0.000$]. Also, differences in EPT scores between the experimental groups were

significant [$F(5,33)=48.678$, $p<0.000$]. Further pairwise tests showed that the EPT values in the untreated axonotomized group (Group 2) were similar to the other axonotomized groups treated with different combinations of PLC membranes and cellular systems (Group 5 and Group 6). The groups treated with cells and PLC membrane (Group 5 and Group 6), however, presented significant differences in EPT values compared to the group treated with PLC membrane only (Group 3) ($p<0.05$), with positive results associated with the cellular system treatment. The group treated with infiltrated undifferentiated HMSCs (Group 4) presented worse recovery of EPT values, when compared to the group where these cells (Group 5 and Group 6) were applied locally, by means of a PLC membrane ($p<0.05$). There were no significant differences between the groups with PLC membranes plus undifferentiated and differentiated HMSCs (Group 5 and Group 6) (Table 2).

3.4.3 Sciatic functional index (SFI)

The SFI score demonstrated severe deficit in the 2 weeks following sciatic nerve crush in all experimental groups. In the following weeks, SFI values improved progressively ending up with values indistinguishable from control animals by week 12 of recovery. Therefore, a significant main effect of time was demonstrated by ANOVA [$F(10,330)=268.937$, $p<0.000$]. ANOVA also demonstrated a significant effect of group [$F(5,33)=52.632$, $p<0.000$]. Further pairwise comparisons located the group effect in the Group 4, with this group displaying delayed recovery of SFI compared to the Group 2 ($p<0.000$) and Group 2 ($p<0.004$) (Table 3).

3.5. Sciatic nerve stereology

Fig. 3 shows the histological appearance of the nerve fibers in the different experimental groups. As expected after a crush injury that does not interrupt the nerve continuity, axon re-generation occurred in all experimental groups. Results of the stereological analysis of regenerated nerve fibers are reported in Table 4. Statistical analysis showed that all axonotmesis groups have a significantly ($p<0.05$) higher number and density of regenerated nerve fibers compared to control. By contrast, in all axonotmesis groups, nerve fibers showed a significantly ($p<0.05$) smaller diameter, of both axon and fiber, and myelin thickness. As far as numerical differences among axonotmesis groups are concerned, statistical analysis did not reveal any significant ($p<0.05$) difference for any of the morphological predictors of nerve recovery except for myelin thickness that was significantly ($p<0.05$) higher in Group 5 and Group 6.

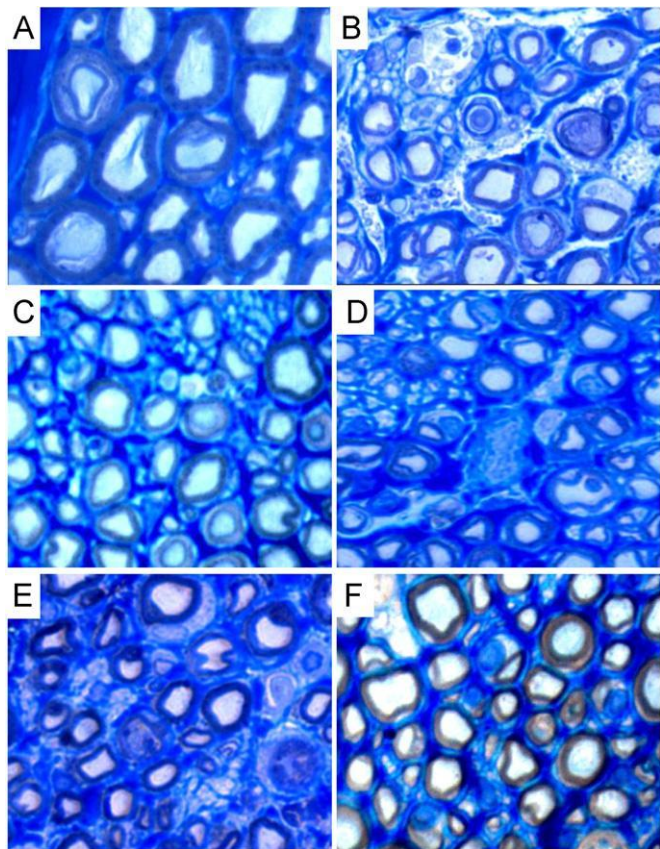


Fig. 3. Histological appearance of the regenerated nerve fibers in the different experimental groups: Control (A), Crush (B), CrushPLC (C), CrushCell (D), Crush-CellNonDifPLC (E), CrushCellDifPLC (F) (Magnification: 1000x).

4. Discussion

Peripheral nerve tissue engineering associates biomaterials to cellular systems, able to differentiate into neuroglial-like cells, which might improve motor and sensory recovery. SCs, MSCs, embryonic stem cells, marrow stromal cells are the most studied support cells candidates. The cellular systems implanted into the injured nerve may produce growth factors or extracellular matrix (ECM) molecules, or may modulate the inflammatory process, to improve nerve regeneration (Amado et al., 2010; Gu et al., 2011; Luis et al., 2007, 2008a; Simoes et al., 2010). To implant cultured cells into defective nerves (with axonotmesis and neurotmesis injuries), there are two main techniques. The cellular system may be directly injected into the neural scaffold which has been interposed between the proximal and distal nerve stumps or around the crush injury (in neurotmesis and axonotmesis injuries, respectively). It can also be performed by pre-adding the cells to the neural scaffold via injection or co-culture (in most of the cellular systems, it is allowed to form a monolayer) and then the biomaterial with the cellular system is implanted in the injured nerve (Maurício et al., 2011).

The majority of natural biomaterials used in clinical applications (for instance, peripheral nerve injuries) such as hyaluronic acid, collagen, and gelatin are derived from animal sources. In spite of thorough purification methods, these materials bear the inherent risk of transfer of viral diseases and may cause immunological body reactions while synthetic biomaterials are not associated with these risks (Maurício et al., 2011). Results obtained from epifluorescence technique that measure the $[Ca^{2+}]_i$ and the cell culture morphology of undifferentiated HMSCs and neuroglial-differentiated HMSCs cul-tured on Vivosorbs membranes evidence that this biomaterial is a viable substrate for undifferentiated HMSCs culture or neuroglial-differentiated HMSCs adhesion, multiplication and differentiation.

Our data showed that PLC does not deleteriously interfere with the nerve regeneration process, as a matter of fact, the informa-tion on the effectiveness of PLC membranes and tube-guides for allowing nerve regeneration was already provided experimentally and with patients (Maurício et al., 2011). PLC becomes hydro-philic by water uptake, which increases the permeability of the polymer. This is important in the control of nutrient and other metabolite transport to the surrounding healing tissue. A few weeks after implantation, the mechanical strength gradually decreases and loss of molecular weight occurs as a result of the hydrolysis process. In approximately 24 months, PLC degrades into lactic acid and hydroxycaproic acid which are both safely metabolized into water and carbon dioxide and/or excreted through the urinary tract. In contrast to other biodegradable polymers, PCL has the advantage of not creating an acidic and potentially disturbing micro-environment, which is favorable to the surrounding tissue (Luis et al., 2007).

Table 4
Histomorphometrical assessment of normal (Group 1—Control) and regenerated sciatic nerves submitted to a standardized sciatic nerve crush injury with non-serrated clamp (week-12 post-traumatic). Results are presented as mean and standard deviation (SD). N corresponds to the number of rats within the experimental group (N¼6).

Group	Fiber density (N/mm2)	Fiber Number (N)	Fiber diameter (lm)	Axon diameter (lm)	Myelin thickness (lm)
Control	15,905 7287	7666 7190	6.6670.12	4.2670.07	1.1970.03
Crush	20,109 71,232	10,644 7423	4.9970.19	3.4870.10	0.7670.05
CrushPLC	23,349 74,278	11,532 71,086	4.5570.36	3.3670.17	0.6070.10
CrushCell	20,200 74,971	9806 72,695	5.3170.69	3.7470.49	0.7870.10
CrushCellNonDiffPLC	20,945 71,162	10,909 71,584	5.1170.42	3.3970.25	0.8670.11
CrushCellDiffPLC	23,593 75,611	9640 71,784	4.9370.43	3.2570.37	0.8470.05

Group 1¼Control (without any sciatic nerve injury), n¼46.

Group 2¼Crush (axonotmesis injury without any other intervention), n¼46.

Group 3¼CrushPLC (axonotmesis lesion of 3 mm enwrapped with a PLC membrane), n¼47.

Group 4¼CrushCell (axonotmesis lesion infiltrated with a suspension of 1250-1500 HMSCs), n¼47.

Group 5¼CrushCellNonDifPLC (axonotmesis lesion of 3 mm enwrapped with a PLC membrane covered with a monolayer of non-differentiated HMSCs), n¼46. Group

6¼CrushCellDiffPLC (axonotmesis lesion of 3 mm enwrapped with a PLC membrane covered with differentiated HMSCs), n¼47.

Extra-embryonic tissues, as stem cell reservoirs, offer many advantages over both embryonic and adult stem cell sources. Extra-embryonic tissues, collectively known as the afterbirth, are routinely discarded at parturition, so little ethical controversy attends the harvest of the resident stem cells populations. Most significantly, the comparatively large volume of extra-embryonic tissues and easy manipulation hypothetically increases the number of stem cells that can be isolated (Marcus and Woodbury, 2008). The UC contains two arteries and one vein protected by a proteoglycan rich connective tissue called Wharton's jelly. Within the abundant extracellular matrix of Wharton's jelly resides a recently described stem cell population. In average, 400,000 cells can be isolated per UC, which is significantly greater than the number of MSCs that can be routinely isolated from adult bone marrow. In vitro, Wharton's jelly MSCs cells are capable of differentiation to multiple mesoderm cell types including skeletal muscle and neurons (Fu et al., 2006; Wang et al., 2004). Generation of clinically important dopaminergic neurons has also been reported (Fu et al., 2006). HMSCs isolated from Wharton's jelly can be easily and ethically obtained and processed compared with embryonic or bone marrow stem cells. These stem cells may be a valuable source in the repair of the peripheral nervous system with capacity to differentiate into neuroglial-like cells (Fu et al., 2006; Yang et al., 2008). The transplanted HMSCs were also able to promote local blood vessel formation and release the neuro-trophic factors brain-derived neurotrophic factor (BDNF) and glial cell line-derived neurotrophic factor (GDNF) (Fu et al., 2006; Wang et al., 2004). Previous results obtained by our research group using N1E-115 cells in vitro differentiated into neuroglial-like cells to promote regeneration of axonotmesis and neurotm-esis lesions in the rat model showed that there was no significant effect in promoting axon regeneration and, when N1E-115 cells were cultured inside a PLGA scaffold used to bridge a nerve defect, they can even exert negative effects on nerve fiber regeneration (Luis et al., 2008a; Maurício et al., 2011). The presence of transplanted N1E-115 cells in nerve scaffolds competing for the local blood supply of nutrients and oxygen and by space-occupying effect could have hindered the positive effect of local neurotrophic factor release leading a negative outcome on nerve regeneration (Amado et al., 2008, 2010; Luis et al., 2008a; Maurício et al., 2011). Thus, N1E-115 cells did not prove to be a suitable candidate cellular system for treatment of nerve injury after axonotmesis and neurotm-esis (Amado et al., 2008, 2010; Luis et al., 2008a; Maurício et al., 2011) and their application is limited only to research purposes as a basic scientific step for the development of other cell delivery systems, due to its neoplastic origin. In this study, we used a PLC membrane to deliver undifferentiated and in vitro differentiated HMSCs from the UC Wharton jelly and we compared this delivery approach with direct infiltration of these undifferentiated HMSCs in suspension, in the rat sciatic nerve axonotmesis model. The cellular systems implanted into the injured nerve may produce growth factors or ECM molecules, or may modulate the inflammatory process, to improve nerve regeneration or even replaced the injured neural and SCs (Amado et al., 2008, 2010; Luis et al., 2008a; Maurício et al., 2011). The differentiated HMSCs karyotype could not be established, once no dividing cells were obtained at passage 5, which can be in agreement with the degree of differentiation. The karyotype analysis of undifferentiated HMSCs previously determined and published elsewhere, excluded the presence of neoplastic signs, thus supporting the suitability of our cell culture and differentiation procedures. This concern also resulted from our previous experience with N1E-115 neoplastic cell line and the negative results we obtained in the treatment of axonotmesis and neurotm-esis injuries (Amado et al., 2008, 2010; Luis et al., 2008b; Maurício et al., 2011). Nevertheless, our cultured undifferentiated HMSCs showed normal morphology when inspected with an inverted microscope. These cells presented a star-like shape with a flat morphology, characteristic of the MSCs.

A consequence of cell metabolism during in vitro expansion and differentiation is that culture conditions are constantly changing. The comprehension and optimization of the expansion and differentiation process of HMSCs will contribute to maximization of cell yield, reduction of cell culture and a decrease of total process costs (Gong et al., 2009; Kirouac and Zandstra, 2008). In culture conditions, cells consume mostly glucose as substrate for the generation of cellular energy (ATP). A high rate of glucose consumption is necessary for cell growth and maintenance. In fact, it has been proposed that cells undergoing high proliferation rates rely essentially on glycolysis to generate ATP, producing considerable amounts of lactate (Vander Heiden et al., 2009). This process, known as Warburg effect, has been described to occur in HMSCs during expansion (Dos Santos et al., 2010; Funes et al., 2007). Our results obtained from the in vitro testing of this cellular system show that during 96 h expansion, the undifferentiated HMSCs consumed glucose and produce, as expected, high concentration of lactate as a metabolic sub-product which is consistent with the Warburg effect and glycolysis stimulation. It was also described that MSCs do not require oxidative phosphorylation to survive (Dos Santos et al., 2010; Funes et al., 2007) instead, hypoxia prolongs the lifespan of these cells, increases their proliferative capacity and reduces differentiation (Fehrer

et al., 2007). Several studies in recent years investigated the biological activity of HMSCs and their in vitro differentiation in neuroglial-like cells (Fu et al., 2004; Mitchell et al., 2003). In this study, HMSCs were in vitro differentiated with neurogenic medium. After 96 h the regular mesenchymal-like shape of the cells changed and the cells became exceedingly long. Morphologically it was observed the formation of neuroglial-like cells after differentiation which were positively stained for the typical specific neuronal markers (Choong et al., 2007; Fu et al., 2004; Mitchell et al., 2003) such as the GFAP, the GAP-43 and the NeuN attesting a clear successful differentiation. The morphologic and biochemical characteristics of neuroglial-like cells are already described but the mechanism by which stem cells differentiate into neuroglial-like cells is still unknown. In our experimental conditions, HMSCs that undergo differentiation in neuroglial-like cells, consumed significantly less glucose and produced significantly less lactate than HMSCs that undergo expansion. These major differences allow us to conclude that during HMSCs differentiation in neuroglial-like cells the glycolytic process, which proved to be the crucial metabolic mechanism during HMSCs expansion, is switched to oxidative metabolism. Several factors, such as inhibition of oxidative phosphorylation due to defects in mitochondrial DNA, dysfunctional Krebs cycle, or inactivation of p53 have been suggested to contribute to the glycolytic switch occurring during cellular expansion and differentiation (Funes et al., 2007). Recently, it has been shown that umbilical-cord derived mesenchymal stem cells adapt their oxygen consumption and energy metabolism to the available oxygen concentrations (Lavrentieva et al., 2010). In our conditions, HMSCs consumed glucose at higher rates during the first 48 h of expansion. After that period the glucose consumption rate decreases although there was no reduction in lactate production rate. Interestingly, during HMSCs differentiation in neuroglial-like cells, lactate production rate is significantly lower and between 72 and 96 h, there was no lactate production rate but rather consumption. The conversion of pyruvate in lactate is an NADH-dependent reduction but pyruvate may also be converted into alanine via transaminase reaction, through the enzyme alanine aminotransaminase (Yang et al., 2002). Surprisingly, during HMSCs expansion, the alanine production significantly increased but the same was not noted during differentiation in neuroglial-like cells. However, the lactate/alanine ratio was lower at 48 and 72 h during HMSCs expansion than at the same periods of differentiation. After 96 h this ratio was decreased in differentiated cells. The appearance of more alanine than lactate in the media of neuroglial-like cells can be associated with a reduced redox cytosolic state (low ratio NADH/NADp) which may point to a role of oxidative stress during the differentiation of HMSCs in neuroglial-like cells, however further investigation is needed to prove this suggestion. Our results show clear evidences that HMSCs expansion is dependent of glycolysis while their differentiation in neuroglial-like cells requires the switch of the metabolic profile to oxidative metabolism. Also important may be the role of oxidative stress during this process.

Here we also tested the efficacy of our combined biomaterial and cellular system approach in the in vivo treatment of sciatic nerve crush injury. Following transection, axons show staggered regeneration and may take substantial time to actually cross the injury site and enter the distal nerve stump (Brushart et al., 2002). Although delayed axonal elongation might be caused by growth inhibition originating from the distal nerve itself, growth-stimulating influences may overcome axons stagger. More robust and fast nerve regeneration is expected to result in better reinnervation and functional recovery. As a potential source of growth promoting signals, HMSCs transplantation is expected to have a positive outcome. Our results showed that the use of either undifferentiated or differentiated HMSCs enhanced the recovery of sensory and motor function. The observation that in both cell-enriched experimental groups myelin sheath was thicker, suggest that HMSCs might exert their positive effects on SCs, the key element in Wallerian degeneration and the following axonal regeneration (Geuna et al., 2009).

5. Conclusion

We conclude that HMSCs isolated from the Wharton's jelly of the UC delivered through PLC membranes might thus be regarded a potentially valuable tool to improve clinical outcome especially after

trauma to sensory nerves, such as digital nerves. In addition, these cells represent a non controversial source of primitive mesenchymal progenitor cells that can be harvested after birth, cryogenically stored, thawed, and expanded for therapeutic uses, including nerve injuries like axonotmesis and neurotmesis.

Funding/suport

This work was supported by Fundac~ao para a Ci~encia e Tecnologia (FCT), Minist~erio da Educac~ao e da Ci~encia, Portugal, through the financed research Project PTDC/DES/104036/2008, by Regione Piemonte, Bando Ricerca Sanitaria Finalizzata and by QREN No. 1372 para Criac~ao de um Nu~cleo I&DT para.

Desenvolvimento de Produtos nas Areas de Medicina Regener-ativa e de Terapias Celulares – Nu~cleo Biomat & Cell. A Gartner has a Doctoral Grant from Fundac~ao para a Ci~encia e Tecnologia (FCT), Minist~erio da Educac~ao e da Ci~encia, Portugal, SFRH/BD/ 70211/2010. PAS Armada-da-Silva is partially supported by a Post-doctoral Grant from Fundac~ao para a Ci~encia e Tecnologia (FCT), Minist~erio da Educac~ao e da Ci~encia, Portugal, SFRH/BPD/ 48489/2008.

Ethical approval

This work is original in that it has not been published before or submitted for publication elsewhere, and will not be submitted elsewhere before a decision has been taken as to its acceptability in this Journal where you are Editor. Each author meets the criteria for authorship and assumes the corresponding responsibility. In this study, laboratory animals were used. All procedures were performed with the approval of the Veterinary Authorities of Portugal in accordance with the European Communities Council Directive of November 1986 (86/609/EEC), and the NIH guidelines for the care and use of laboratory animals have been observed.

Acknowledgments

The authors would like to gratefully acknowledge the valuable support by of Jose Manuel Correia Costa, from Laborat~orio de Parasitologia, Instituto Nacional de Sau~de Dr. Ricardo Jorge (INSRJ), Porto, Portugal. The authors would also like to gratefully acknowl-edge Simone Bompasso for the technical assistance for the histo-logical processing of tissues.

References

Amado, S., Rodrigues, J.M., Luis, A.L., Armada-da-Silva, P.A., Vieira, M., Gartner, A., Simoes, M.J., Veloso, A.P., Fornaro, M., Raimondo, S., Varejao, A.S., Geuna, S., Mauricio, A.C., 2010. Effects of collagen membranes enriched with in vitro-differentiated N1E-115 cells on rat sciatic nerve regeneration after end-to-end repair. *Journal of NeuroEngineering and Rehabilitation* 7, 7.

Amado, S., Simoes, M.J., Armada da Silva, P.A., Luis, A.L., Shirosaki, Y., Lopes, M.A., Santos, J.D., Fregnan, F., Gambarotta, G., Raimondo, S., Fornaro, M., Veloso, A.P., Varejao, A.S., Mauricio, A.C., Geuna, S., 2008. Use of hybrid chitosan membranes and N1E-115 cells for promoting nerve regeneration in an axonotmesis rat model. *Biomaterials* 29, 4409–4419.

Bain, J.R., Mackinnon, S.E., Hunter, D.A., 1989. Functional evaluation of complete sciatic, peroneal, and posterior tibial nerve lesions in the rat. *Plastic and Reconstructive Surgery* 83, 129–138.

Bhatheja, K., Field, J., 2006. Schwann cells: origins and role in axonal maintenance and regeneration.

The International Journal of Biochemistry & Cell Biology 38, 1995–1999.

Brushart, T.M., Hoffman, P.N., Royall, R.M., Murinson, B.B., Witzel, C., Gordon, T., 2002. Electrical stimulation promotes motoneuron regeneration without increasing its speed or conditioning the neuron. *Journal of Neuroscience* 22, 6631–6638.

Chen, C.-J., Ou, Y.-C., Liao, S.-L., Chen, W.-Y., Chen, S.-Y., Wu, C.-W., Wang, C.-C., Wang, W.-Y., Huang, Y.-S., Hsu, S.-H., 2007. Transplantation of bone marrow stromal cells for peripheral nerve repair. *Experimental Neurology* 204, 443–453.

Choong, P.F., Mok, P.L., Cheong, S.K., Leong, C.F., Then, K.Y., 2007. Generating neuron-like cells from BM-derived mesenchymal stromal cells in vitro. *Cytotherapy* 9, 170–183.

Colter, D.C., 2000. Rapid expansion of recycling stem cells in cultures of plastic-adherent cells from human bone marrow. *Proceedings of the National Academy of Sciences* 97, 3213–3218.

Dezawa, M., Takahashi, I., Esaki, M., Takano, M., Sawada, H., 2001. Sciatic nerve regeneration in rats induced by transplantation of in vitro differentiated bone-marrow stromal cells. *European Journal of Neuroscience* 14, 1771–1776.

Dijkstra, J.R., Meek, M.F., Robinson, P.H., Gramsbergen, A., 2000. Methods to evaluate functional nerve recovery in adult rats: walking track analysis, video analysis and the withdrawal reflex. *Journal of Neuroscience Methods* publishes 96, 89–96.

Dos Santos, F., Andrade, P.Z., Boura, J.S., Abecasis, M.M., da Silva, C.L., Cabral, J.M., 2010. Ex vivo expansion of human mesenchymal stem cells: a more effective cell proliferation kinetics and metabolism under hypoxia. *Journal of Cellular Physiology* 223, 27–35.

Fansa, H., Keilhoff, G., Plogmeier, K., Frerichs, O., Wolf, G., Schneider, W., 1999. Successful implantation of Schwann cells in acellular muscles. *Journal of Reconstructive Microsurgery* 15, 61–65.

Fehrer, C., Brunauer, R., Laschober, G., Unterluggauer, H., Reitinger, S., Kloss, F., Gully, C., Gassner, R., Lepperdinger, G., 2007. Reduced oxygen tension attenuates differentiation capacity of human mesenchymal stem cells and prolongs their lifespan. *Aging Cells* 6, 745–757.

Fu, Y.-S., Cheng, Y.-C., Lin, M.-Y.A., Cheng, H., Chu, P.-M., Chou, S.-C., Shih, Y.-H., Ko, M.-H., Sung, M.-S., 2006. Conversion of human umbilical cord mesenchymal stem cells in Wharton's jelly to dopaminergic neurons in vitro: potential therapeutic application for Parkinsonism. *Stem Cells* 24, 115–124.

Fu, Y.-S., Shih, Y.-T., Cheng, Y.-C., Min, M.-Y., 2004. Transformation of human umbilical mesenchymal cells into neurons in vitro. *Journal of Biomedical Science* 11, 652–660.

Funes, J.M., Quintero, M., Henderson, S., Martinez, D., Qureshi, U., Westwood, C., Clements, M.O., Bourboulia, D., Pedley, R.B., Moncada, S., Boshoff, C., 2007. Transformation of human mesenchymal stem cells increases their dependency on oxidative phosphorylation for energy production. *Proceedings of the National Academy of Sciences USA* 104, 6223–6228.

Geuna, S., Gigo-Benato, D., Rodrigues Ade, C., 2004. On sampling and sampling errors in histomorphometry of peripheral nerve fibers. *Microsurgery* 24, 72–76.

Geuna, S., Raimondo, S., Ronchi, G., Di Scipio, F., Tos, P., Czaja, K., Fornaro, M., 2009. Histology of the peripheral nerve and changes occurring during nerve regeneration. *International Review of Neurobiology* 87, 27–46.

Geuna, S., Tos, P., Battiston, B., Guglielmone, R., 2000. Verification of the two-dimensional disector, a method for the unbiased estimation of density and number of myelinated nerve fibers in peripheral nerves. *Annals of Anatomy* 182, 23–34.

Gnecchi, M., Melo, L.G., 2009. Bone marrow-derived mesenchymal stem cells: isolation, expansion, characterization, viral transduction, and production of conditioned medium. *Methods of Molecular Biology* 482, 281–294.

Gong, Z., Calkins, G., Cheng, E.C., Krause, D., Niklason, L.E., 2009. Influence of culture medium on smooth muscle cell differentiation from human bone marrow-derived mesenchymal stem cells. *Tissue Engineering Part A* 15, 319–330.

Gu, X., Ding, F., Yang, Y., Liu, J., 2011. Construction of tissue engineered nerve grafts and their application in peripheral nerve regeneration. *Progress in Neuro-biology* 93, 204–230.

Hall, S.M., 1978. The schwann cell: a reappraisal of its role in the peripheral nervous system. *Neuropathology and Applied Neurobiology* 4, 165–176.

Hu, D., Hu, R., Berde, C.B., 1997. Neurologic evaluation of infant and adult rats before and after sciatic nerve blockade. *Anesthesiology* 86, 957–965.

Ide, C., 1996. Peripheral nerve regeneration. *Neuroscience Research* 25, 101–121. Joshi, C.V., Enver, T., 2002. Plasticity revisited. *Current Opinion in Cell Biology* 14,

749–755.

Keilhoff, G., Goihl, A., Langnase, K., Fansa, H., Wolf, G., 2006. Transdifferentiation of mesenchymal stem cells into Schwann cell-like myelinating cells. *European Journal of Cell Biology* 85, 11–24.

Kirouac, D.C., Zandstra, P.W., 2008. The systematic production of cells for cell therapies. *Cell Stem Cell* 3, 369–381.

Koka, R., Hadlock, T.A., 2001. Quantification of functional recovery following rat sciatic nerve transection. *Experimental Neurology* 168, 192–195.

Ladak, A., Olson, J., Tredget, E.E., Gordon, T., 2011. Differentiation of mesenchymal stem cells to

support peripheral nerve regeneration in a rat model. *Experimental Neurology* 228, 242–252.

Lavrentieva, A., Majore, I., Kasper, C., Hass, R., 2010. Effects of hypoxic culture conditions on umbilical cord-derived human mesenchymal stem cells. *Cell Communication and Signaling* 8, 18.

Luis, A.L., Amado, S., Geuna, S., Rodrigues, J.M., Simoes, M.J., Santos, J.D., Fregnan, F., Raimondo, S., Veloso, A.P., Ferreira, A.J.A., Armada-da-Silva, P.A.S., Varejao, A.S.P., Mauricio, A.C., 2007. Long-term functional and morphological assessment of a standardized rat sciatic nerve crush injury with a non-serrated clamp. *Journal of Neuroscience Methods* 163, 92–104.

Luis, A.L., Rodrigues, J.M., Amado, S., Veloso, A.P., Armada-Da-Silva, P.A., Raimondo, S., Fregnan, F., Ferreira, A.J., Lopes, M.A., Santos, J.D., Geuna, S., Varejao, A.S., Mauricio, A.C., 2007. PLGA 90/10 and caprolactone biodegradable nerve guides for the reconstruction of the rat sciatic nerve. *Microsurgery* 27, 125–137.

Luis, A.L., Rodrigues, J.M., Geuna, S., Amado, S., Shirosaki, Y., Lee, J.M., Fregnan, F., Lopes, M.A., Veloso, A.P., Ferreira, A.J., Santos, J.D., Armada-Da-silva, P.A., Varejao, A.S., Mauricio, A.C., 2008a. Use of PLGA 90:10 scaffolds enriched with in vitro-differentiated neural cells for repairing rat sciatic nerve defects. *Tissue Engineering Part A* 14, 979–993.

Luis, A.L., Rodrigues, J.M., Geuna, S., Amado, S., Simoes, M.J., Fregnan, F., Ferreira, A.J., Veloso, A.P., Armada-da-Silva, P.A., Varejao, A.S., Mauricio, A.C., 2008b. Neural cell transplantation effects on sciatic nerve regeneration after a standardized crush injury in the rat. *Microsurgery* 28, 458–470.

Mackinnon, S.E., Hudson, A.R., Hunter, D.A., 1985. Histologic assessment of nerve regeneration in the rat. *Plastic and Reconstructive Surgery* 75, 384–388.

Madduri, S., Gander, B., 2010. Schwann cell delivery of neurotrophic factors for peripheral nerve regeneration. *Journal of Peripheral Nervous System* 15, 93–103.

Marcus, A.J., Woodbury, D., 2008. Fetal stem cells from extra-embryonic tissues: do not discard. *Journal of Cellular and Molecular Medicine* 12, 730–742.

Masters, D.B., Berde, C.B., Dutta, S.K., Griggs, C.T., Hu, D., Kupsky, W., Langer, R., 1993. Prolonged regional nerve blockade by controlled release of local anesthetic from a biodegradable polymer matrix. *Anesthesiology* 79, 340–346.

Mauricio, A.C., Gartner, A., Armada-da-Silva, P., Amado, S., Pereira, T., Veloso, A.P., Vareja*o, A., Luis, A.L., Geuna, S., 2011. Cellular Systems and Biomaterials for Nerve Regeneration in Neurotmesis Injuries, in: Pignatello, R. (Ed.), *Biomaterials Applications for Nanomedicine*, ISBN: 978-953-307-661-4, Available from: InTech.

Mitchell, K.E., Weiss, M.L., Mitchell, B.M., Martin, P., Davis, D., Morales, L., Helwig, B., Beerenstrauch, M., Abou-Easa, K., Hildreth, T., Troyer, D., Medicetty, S., 2003. Matrix cells from

Wharton's jelly form neurons and glia. *Stem Cells* 21, 50–60.

Muir, D., 2010. The potentiation of peripheral nerve sheaths in regeneration and repair. *Experimental Neurology* 223, 102–111.

Park, H.-W., Lim, M.-J., Jung, H., Lee, S.-P., Paik, K.-S., Chang, M.-S., 2010. Human mesenchymal stem cell-derived Schwann cell-like cells exhibit neurotrophic effects, via distinct growth factor production, in a model of spinal cord injury. *Glia* 58, 1118–1132.

Raimondo, S., Fornaro, M., Di Scipio, F., Ronchi, G., Giacobini-Robecchi, M.G., Geuna, S., 2009. Methods and protocols in peripheral nerve regeneration experimental research: part II-morphological techniques. *International Review of Neurobiology* 87, 81–103.

Ronchi, G., Nicolino, S., Raimondo, S., Tos, P., Battiston, B., Papalia, I., Varejao, A.S.P., Giacobini-Robecchi, M.G., Perroteau, I., Geuna, S., 2009. Functional and morphological assessment of a standardized crush injury of the rat median nerve. *Journal of Neuroscience Methods* 179, 51–57.

Sarugaser, R., Lickorish, D., Baksh, D., Hosseini, M.M., Davies, J.E., 2005. Human umbilical cord perivascular (hucpv) cells: a source of mesenchymal progenitors. *Stem Cells* 23, 220–229.

Schlosshauer, B., Muller, E., Schroder, B., Planck, H., Muller, H.W., 2003. Rat Schwann cells in bioresorbable nerve guides to promote and accelerate axonal regeneration. *Brain Research* 963, 321–326.

Schmitte, R., Tipold, A., Stein, V.M., Schenk, H., Flieshardt, C., Grothe, C., Haastert, K., 2010. Genetically modified canine Schwann cells—In vitro and in vivo evaluation of their suitability for peripheral nerve tissue engineering. *Journal of Neuroscience Methods* 186, 202–208.

Scipio, F.D., Raimondo, S., Tos, P., Geuna, S., 2008. A simple protocol for paraffinembedded myelin sheath staining with osmium tetroxide for light microscope observation. *Microscopy Research and Technique* 71, 497–502.

Simoes, M.J., Amado, S., Gartner, A., Armada-Da-Silva, P.A., Raimondo, S., Vieira, M., Luis, A.L., Shirosaki, Y., Veloso, A.P., Santos, J.D., Varejao, A.S., Geuna, S., Mauricio, A.C., 2010. Use of chitosan scaffolds for repairing rat sciatic nerve defects. *Italian Journal of Anatomy and Embryology* 115, 190–210.

Thuret, S., Moon, L.D.F., Gage, F.H., 2006. Therapeutic interventions after spinal cord injury. *Nature Reviews Neuroscience* 7, 628–643.

Tohill, M., Mantovani, C., Wiberg, M., Terenghi, G., 2004. Rat bone marrow mesenchymal stem cells express glial markers and stimulate nerve regeneration. *Neuroscience Letters* 362, 200–203.

Vander Heiden, M.G., Cantley, L.C., Thompson, C.B., 2009. Understanding the Warburg effect: the metabolic requirements of cell proliferation. *Science* 324, 1029–1033.

Varejao, A.S., Cabrita, A.M., Geuna, S., Patricio, J.A., Azevedo, H.R., Ferreira, A.J., Meek, M.F., 2003. Functional assessment of sciatic nerve recovery: biodegradable poly (DLA-epsilon-CL) nerve guide filled with fresh skeletal muscle. *Microsurgery* 23, 346–353.

Wang, H.-S., Hung, S.-C., Peng, S.-T., Huang, C.-C., Wei, H.-M., Guo, Y.-J., Fu, Y.-S., Lai, M.-C., Chen, C.-C., 2004. Mesenchymal stem cells in the Wharton's Jelly of the human umbilical cord. *Stem Cells* 22, 1330–1337.

Weiss, M.L., Medicetty, S., Bledsoe, A.R., Rachakatla, R.S., Choi, M., Merchav, S., Luo, Y., Rao, M.S., Velagaleti, G., Troyer, D., 2006. Human umbilical cord matrix stem cells: preliminary characterization and effect of transplantation in a rodent model of Parkinson's disease. *Stem Cells* 24, 781–792.

Weiss, M.L., Mitchell, K.E., Hix, J.E., Medicetty, S., El-Zarkouny, S.Z., Grieger, D., Troyer, D.L., 2003. Transplantation of porcine umbilical cord matrix cells into the rat brain. *Experimental Neurology* 182, 288–299.

Yang, C.C., Shih, Y.H., Ko, M.H., Hsu, S.Y., Cheng, H., Fu, Y.S., 2008. Transplantation of human umbilical mesenchymal stem cells from Wharton's jelly after complete transection of the rat spinal cord. *PLoS One* 3, e3336.

Yang, R.Z., Blaileanu, G., Hansen, B.C., Shuldiner, A.R., Gong, D.W., 2002. cDNA cloning, genomic structure, chromosomal mapping, and functional expression of a novel human alanine aminotransferase. *Genomics* 79, 445–450.